Geoscience Frontiers 16 (2025) 102178

Contents lists available at ScienceDirect

Geoscience Frontiers

journal homepage: www.elsevier.com/locate/gsf

Research Paper

Spatiotemporal analysis of the FWI over Europe and North Africa: Historical trends and climate projections under RCP4.5 and RCP8.5

Fabio Di Nunno *, Francesco Granata

University of Cassino and Southern Lazio, Department of Civil and Mechanical Engineering (DICEM), Via Di Biasio, 43, Cassino, Frosinone 03043, Italy

ARTICLE INFO

Article history:
Received 31 May 2025
Revised 29 August 2025
Accepted 2 October 2025
Available online 7 October 2025

Keywords:
Climate change
Fire weather index
Global climate models
Trend analysis

ABSTRACT

Wildfires represent an escalating environmental threat across Europe and North Africa, increasingly exacerbated by climate-driven shifts in temperature, precipitation, and drought patterns. However, there is still limited large-scale, methodologically consistent research that simultaneously assesses historical patterns and future projections of fire danger across these regions, particularly in terms of both frequency and duration of risk under different climate scenarios. This study addresses this gap by providing a high-resolution, spatiotemporal assessment of fire weather conditions, with the aim of offering critical insights to support climate-adaptive fire management strategies, extended preparedness frameworks, and the integration of future fire weather projections into land-use and risk governance policies. To achieve this, we investigate historical (1979–2021) and projected (2000–2098) trends in fire danger using the Canadian Fire Weather Index (FWI), based on ERA5 reanalysis data and outputs from five Global Climate Models (GCMs) under RCP4.5 and RCP8.5 scenarios. Over 50,000 land grid cells were analyzed to assess the frequency and duration of six FWI danger classes. Different metrics were used to quantify the agreement between historical reanalysis data and GCM outputs, while the Seasonal Kendall (SK) test was applied to detect trends. Results reveal a substantial decline in the duration of the very low FWI class, from 36 to 23 months, and significant increases in both the duration and frequency of the extreme FWI class, reaching up to 6.38 months and 14.42% under the RCP8.5 scenario. Correlation coefficients exceed 0.8 across much of Southern Europe and North Africa, indicating strong temporal agreement. Trend analyses reveal statistically significant increases in fire danger across southern latitudes, while Northern Europe shows mixed or decreasing trends. These findings project a dramatic intensification and expansion of fire-prone conditions, particularly under high-emission scenarios.

1. Introduction

Wildfires have increasingly become a symbol of the growing environmental challenges confronting the 21st century, causing significant ecological, economic, and societal damage worldwide (Abatzoglou et al., 2019). This upsurge in wildfire frequency and severity is largely attributed to shifting climatic patterns—rising global temperatures, prolonged drought periods, and erratic precipitation regimes—which are fundamentally reshaping ecosystems and elevating fire risk across regions (Pinto et al., 2020; Calheiros et al., 2021).

Among the most vulnerable to these changes is the European-Mediterranean region, encompassing Southern Europe and North Africa. This area is characterized by complex topography, diverse land use practices, and the Mediterranean climate's inherently dry summers. Together, these factors converge to intensify baseline fire susceptibility. Climate change exacerbates this vulnerability, as evidenced by the growing frequency and magnitude of extreme fire weather events (Cane et al., 2008; Carvalho et al., 2011; Bedia et al., 2018). In recent years, severe wildfire outbreaks in countries such as Greece, Spain, Portugal, Algeria, and Turkey have led to large-scale evacuations, significant fatalities, and widespread economic and environmental losses (Rovithakis et al., 2022; Zaidi, 2023; Avcıoğlu et al., 2025; Senande-Rivera et al., 2025). A parallel can be drawn with the devastating wildfires in California in 2023 and 2025, including those around the Los Angeles area, which resulted in massive evacuations, loss of life, and multi-billion-dollar damages (Horing et al., 2025).

Central to monitoring and forecasting wildfire risk is the Fire Weather Index (FWI), a widely adopted, dimensionless numerical

* Corresponding author.
E-mail addresses: fabio.dinunno@unicas.it (F. Di Nunno), f.granata@unicas.it (F. Granata).

https://doi.org/10.1016/j.gsf.2025.102178

rating that estimates potential wildfire intensity based on meteorological conditions (Field, 2020). Initially developed for operational, short-term fire danger rating, the FWI is now frequently used in long-term analyses to identify trends in fire-prone conditions. However, its deterministic structure and empirical thresholds may not fully capture the non-linear and accelerating dynamics of fire regimes under anthropogenic climate change (Abatzoglou and Williams, 2016; Goss et al., 2020). Contemporary research reveals that global warming is not only amplifying fire weather intensity but also shifting the timing, duration, and spatial distribution of fire seasons (Jain et al., 2022). Raising questions about the FWI's adequacy as a tool for scenario-based projections.

Globally, climate change is reshaping rainfall and temperature regimes, with growing evidence of hydroclimatic instability. In Bihar, India, Kumar and Thangavel (2025) reported increasing pre-monsoon rainfall and declining monsoon precipitation, with clear change points in seasonal patterns. Similar disruptions were observed in Madhya Pradesh, where rainfall variability intensified after 1998 (Kumar et al., 2023a), and long-term warming trends, especially in winter, were detected (Kumar et al., 2023b). Using integrated statistical and GIS tools, Kumar et al. (2024) further mapped spatial shifts in climate variables across the region.

In South America, recent studies highlight a concurrent rise in warming, drought, and fire risk, particularly in regions such as the northern Amazon and the Gran Chaco. Feron et al. (2024) demonstrated a threefold increase in days with extreme fire weather, characterized by high temperatures, low humidity, and dryness, since 1971, driven by both anthropogenic warming and ocean–atmosphere interactions like El Niño and La Niña events.

Further illustrating the global scale of fire risk intensification, Richardson et al. (2025) demonstrated that the historically asynchronous fire seasons of Australia and North America are now increasingly overlapping due to prolonged fire weather in both regions. Their analysis, based on the Canadian Fire Weather Index and CMIP6 ensemble projections, found the overlap has grown by roughly one day per year since 1979 and could increase by up to 29 days annually by 2050, posing serious challenges for international firefighting cooperation and resource allocation.

By incorporating such insights from South Asia, South America, and the Pacific regions, this study situates European-Mediterranean wildfire dynamics within a broader global framework. Changes in rainfall and temperature across continents contribute to increased fuel aridity, extended fire seasons, and shifting fire regimes. Understanding wildfire danger under climate change therefore demands a globally contextualized view of hydroclimatic variability and extremes.

Given the increasing complexity of wildfire dynamics under climate change, there is a critical need to reassess fire danger trends using climate-informed modeling approaches. Although numerous studies have examined fire weather trends at national or subregional scales, few have provided a systematic, large-scale evaluation that spans both Europe and North Africa using a consistent methodological framework. There remains a gap in understanding how future fire weather regimes, characterized by both the frequency and duration of fire danger, will evolve across diverse climatic zones under different greenhouse gas emission scenarios. Furthermore, the ability of current climate models to replicate historical fire danger variability has not been sufficiently explored on a transcontinental scale.

This study addresses existing gaps by providing a data-driven, high-resolution spatiotemporal assessment of fire weather conditions across Europe and North Africa. The primary objectives are to: (1) characterize historical trends in fire danger using monthly FWI data from the ERA5-Land reanalysis; (2) evaluate long-term projections of fire danger under two future climate scenarios (RCP4.5 and RCP8.5) based on five state-of-the-art GCMs; (3) assess the consistency between historical and modeled data through various metrics during their overlapping periods.

The analysis covers over 50,000 land-based grid cells, allowing a comprehensive characterization of trends in both the duration and frequency of fire danger across diverse geographic and climatic regions. To detect trends while accounting for seasonal variation and the non-normality inherent in climate time series, the Seasonal Kendall (SK) test was applied. This methodological framework supports a robust and spatially explicit understanding of how fire danger may evolve under continued global warming and provides a foundation for future scenario-based risk assessments and policy planning.

2. Materials and methods

2.1. Study area

This study encompasses the European continent and the adjoining North African region, collectively representing a vast and ecologically diverse domain with pronounced climatic and environmental gradients. Europe, stretching from the maritime climates of the Atlantic coast to the continental interiors and the boreal zones of the north, exhibits significant variation in fire susceptibility due to differing seasonal precipitation regimes, vegetation types, and land-use practices. In contrast, North Africa is dominated by arid and semi-arid landscapes, where extreme heat, scarce rainfall, and persistent drought conditions converge to create a highly fire-prone environment.

The inclusion of both Europe and North Africa enables a transcontinental analysis of FWI under a range of current and projected climate conditions. This spatially expansive framework captures the dynamic interactions between Mediterranean, Atlantic, and desert climate influences, offering a comprehensive perspective on how fire weather patterns may evolve across latitudes. Given the anticipated amplification of climate extremes, such as prolonged dry spells, intense heatwaves, and altered wind patterns, this cross-regional approach is critical for understanding emerging wildfire risks and supporting adaptive fire management strategies across contrasting biogeographical zones.

2.2. Dataset

FWI integrates measurements of four key variables—air temperature, relative humidity, wind speed and precipitation—into a composite metric indicating fire potential. Specifically, the FWI system comprises six components: three fuel moisture codes, Fine Fuel Moisture Code (FFMC), Duff Moisture Code (DMC), and Drought Code (DC), which represent the moisture content of different forest floor layers; and three fire behavior indices, Initial Spread Index (ISI), Buildup Index (BUI), and the Fire Weather Index (FWI) itself. The FFMC is calculated using temperature, precipitation, wind speed, and relative humidity. The DMC uses temperature, precipitation, and relative humidity, while the DC relies on temperature and precipitation. The ISI combines FFMC and wind speed, and the BUI combines DMC and DC. Finally, the FWI integrates ISI and BUI to provide a comprehensive measure of potential fire intensity (Bedia et al., 2013).

This study employs a combination of historical reanalysis data and future climate projections. The historical dataset consists of gridded monthly FWI values derived from the ERA5 reanalysis product, developed by the European Centre for Medium-Range Weather Forecasts (ECMWF) and disseminated through the Copernicus Climate Data Store. As a core component of the Canadian Forest Fire Weather Index System, the FWI synthesizes key meteorological variables—air temperature, relative humidity, wind

speed, and accumulated precipitation—into a single metric indicative of fire potential. This index is extensively utilized for operational fire risk assessments across Europe and globally.

The ERA5-based dataset spans the period from January 1979 to December 2021, representing the most complete temporal coverage currently available. Data are provided at a horizontal resolution of 0.25° × 0.25°, encompassing the entire European continent and North Africa. After excluding oceanic grid cells and land points with incomplete records, the final dataset comprises a spatially consistent gridded time series of monthly mean FWI values of 50,135 grid cells.

To extend the temporal horizon of the analysis, future FWI values were also considered under the scenarios RCP4.5 and RCP8.5, over the period from January 2000 to December 2098. These projections are derived from five GCMs, all of which are part of the Coupled Model Intercomparison Project Phase 5 (CMIP5): Centre National de Recherches Météorologiques – Coupled Model version 5 (CNRM-CM5, developed by CNRM-CERFACS, France), European Consortium Earth System Model (EC-EARTH, developed by the Irish Centre for High-End Computing, ICHEC, Ireland), Institut Pierre-Simon Laplace – Coupled Model version 5A, Medium Resolution (IPSL-CM5A-MR, developed by IPSL, France), Hadley Centre Global Environment Model version 2 – Earth System (HadGEM2-ES, developed by the UK Met Office, United Kingdom), and Max Planck Institute Earth System Model, Low Resolution (MPI-ESM-LR, developed by the Max Planck Institute for Meteorology, Germany). These models simulate interactions between the atmosphere, oceans, land surface, and cryosphere, and are widely used in climate impact studies. Each GCM has specific strengths and structural differences. For instance, HadGEM2-ES includes an interactive carbon cycle and is known for its relatively high climate sensitivity (Caesar et al., 2013), whereas MPI-ESM-LR offers stable long-term simulations with a well-balanced energy budget, as demonstrated in its comprehensive evaluation for CMIP5 (Giorgetta et al., 2013). EC-EARTH emphasizes European climate processes and has been effectively employed in regional climate studies, benefiting from its flexible coupling framework and improved physical performance over its predecessors (Döscher et al., 2022). The IPSL-CM5A-MR model offers enhanced spatial resolution and demonstrates improved simulation of temperature and precipitation variability, particularly across the Mediterranean region (Dufresne et al., 2013). Similarly, CNRM-CM5 has shown strong performance in simulating temperature and precipitation patterns in the Mediterranean area, contributing valuable insights into regional climate dynamics (Voldoire et al., 2013). Employing a multi-model ensemble approach in this study helps account for structural uncertainties and enhances the robustness of future projections.

By combining historical reanalysis data from ERA5 with multi-scenario climate projections from CMIP5 models, this study enables a consistent and comprehensive investigation of FWI trends across diverse climatic regimes and extended temporal scales. This integrated framework is essential for assessing the evolving nature of wildfire risk under anthropogenic climate change, as it captures both past variability and plausible future trajectories of fire weather conditions.

Finally, FWI is commonly classified into six categories of fire danger, following the scheme adopted by the European Forest Fire Information System (EFFIS). These classes range from very low danger when the FWI is below 5.2, to low danger for values between 5.2 and 11.2, and moderate danger when the index lies between 11.2 and 21.3. The category of high danger is assigned to values from 21.3 to 38.0, followed by very high danger between 38.0 and 50.0. Finally, FWI values exceeding 50 are considered indicative of extreme danger.

Fig. 1 presents the mean and standard deviation of the Fire Weather Index (FWI) for the historical time series, computed separately for the four climatological seasons: December–February (DJF), March–May (MAM), June–August (JJA), and September–November (SON). During winter (DJF), mean FWI values remain very low across most of Europe, with only localized increases in North Africa and parts of southern Spain and Greece. In spring (MAM), FWI begins to rise across the Mediterranean basin, with notable gradients between southern and northern Europe. Summer (JJA) shows the highest FWI values, concentrated over the Mediterranean coasts, North Africa, and large areas of Central and Northern Europe, indicating peak fire–weather conditions. Autumn (SON) maintains elevated FWI in southern Europe and North Africa, though values decrease across central and northern regions. The standard deviation shows a comparable seasonal pattern, remaining low in DJF and MAM but increasing markedly in JJA and SON, particularly across the Mediterranean and Northern Africa. This indicates more variable and occasionally extreme fire–weather conditions during the warmer seasons.

2.3. Modeling procedure

To characterize the evolution of fire danger under changing climate conditions, this study evaluates both the duration and frequency of FWI occurrences within each danger class (very low to extreme). Duration refers to the maximum number of consecutive months a given grid cell remains within a specific FWI category, while frequency indicates the total number of months per year classified within that category, regardless of sequence. These metrics are computed for both the historical baseline period (1979–2021) and the future projections (2000–2098) under RCP4.5 and RCP8.5, across all five GCMs. The comparative analysis enables a systematic assessment of temporal shifts in fire weather regime persistence and recurrence across the study area.

To assess the degree of statistical agreement between historical reanalysis data and GCM-based projections, a cross-correlation analysis was conducted. For each GCM and RCP scenario, the overlapping period with GCM data (2000–2021) was identified, and different metrics were calculated between the observed and simulated FWI time series. This procedure provides an initial quantitative measure of temporal coherence and supports the identification of potential biases or structural discrepancies across the models prior to long-term evaluation. Similar overlap-period assessments and continuity checks have been applied in recent climate-model evaluation studies (McBride et al., 2021; Berio Fortini et al., 2023). Metrics include: Correlation Coefficient (r), Willmott's Index of Agreement (WI), Kling-Gupta Efficiency (KGE), Root Mean Square Error (RMSE), Mean Absolute Error (MAE), and Relative Absolute Error (RAE). A detailed description of the metrics is given in Supplementary Data Table S1.

Overall, the combination of statistical metrics provides a robust and comprehensive assessment of model performance. While the correlation coefficient captures the agreement in temporal patterns, RMSE and MAE reflect differences in magnitude, with MAE offering a more interpretable average error. The WI and KGE further enhance diagnostic power by accounting for both linear and nonlinear discrepancies, and RAE offers a normalized measure of error relative to a naïve baseline. Together, these complementary metrics ensure that both structural and quantitative aspects are thoroughly evaluated, making them well-suited for assessing consistency between historical data and GCM projections.

Finally, the SK test was selected due to its ability to account for seasonal variations in time series data, addressing the limitations of traditional approaches such as the Mann-Kendall (MK) test, which often fail to adequately represent the seasonality inherent

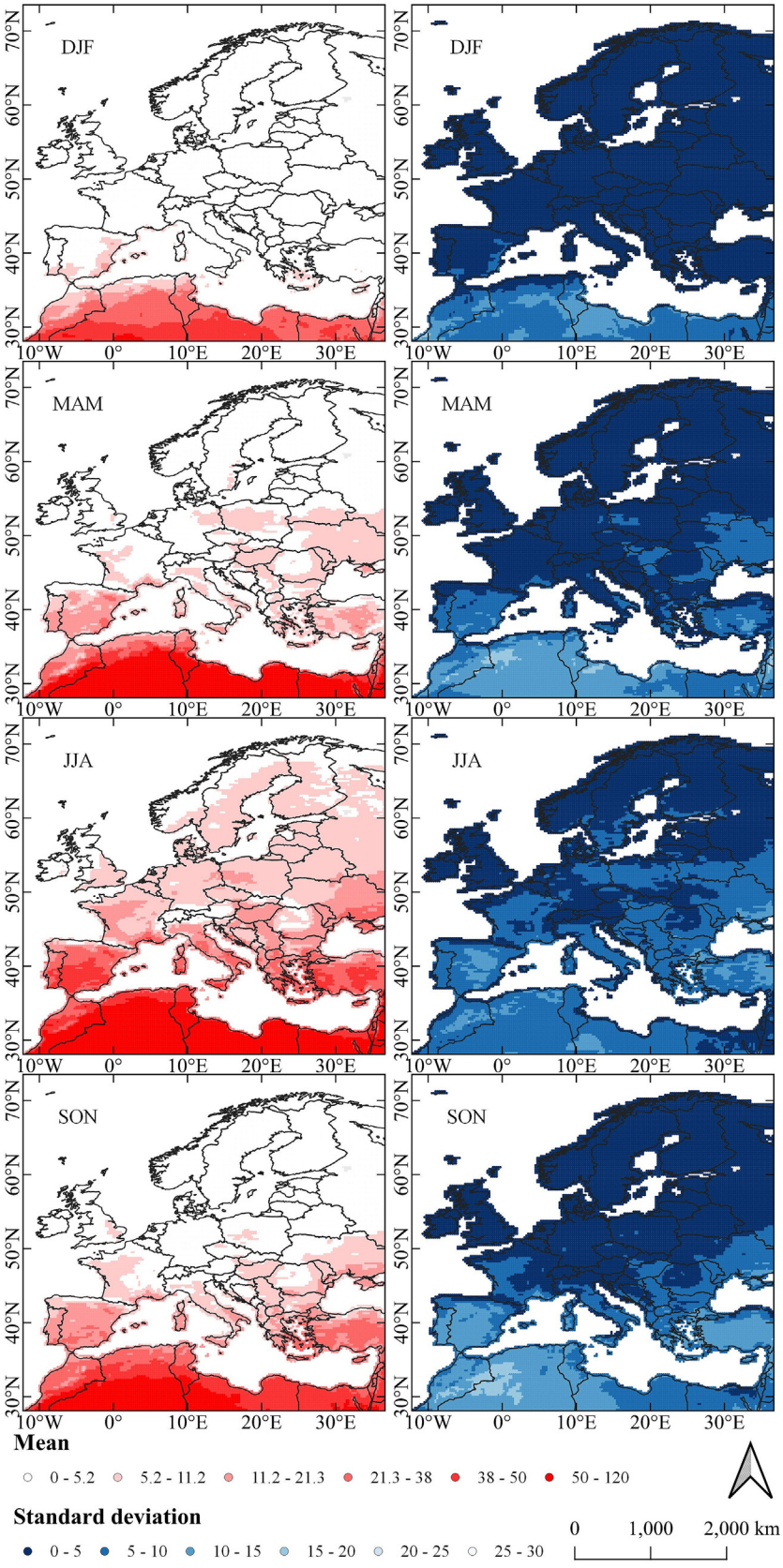

Fig. 1. Mean and standard deviation of FWI for the historical time series computed for the four seasons: December–January–February (DJF), March–April–May (MAM), June–July–August (JJA), and September–October–November (SON).

in climate-related variables like the FWI. The SK test is particularly well-suited for variables characterized by strong interannual variability and non-normal distributions. The SK test was applied independently to each grid cell in both historical and future FWI datasets, allowing for a spatially explicit assessment of monotonic trends. Given the focus on monthly-scale FWI variations, the statistic S was computed separately for each of the m months (S_m), with the overall statistic S_S defined as:

$$S_s = \sum_{m=1}^{p=12} S_m \tag{1}$$

The longer the time series, the better the distribution of S_S can be approximated by a normal distribution, and therefore it can be standardized as:

$$Z = \begin{cases} \frac{S_S-1}{\sigma_S}, & S_S > 0 \\ 0, & S_S = 0 \\ \frac{S_S+1}{\sigma_S}, & S_S < 0 \end{cases} \tag{2}$$

where σ_S is the standard deviation of S_S, computed as:

$$\sigma_S = \sqrt{\sum_{m=1}^{p} \frac{n_p}{18}(n_p - 1)(2n_p + 5)} \tag{3}$$

with n_p is the number of values in season m and p is the number of seasons, equal to 12 months for the present study. The Z value is used to detect a statistically significant trend. Two strict confidence thresholds were adopted to ensure statistical robustness: Z = ±1.96 ($p \leq 0.05$, significant at the 95% confidence level) and Z = ±2.576 ($p \leq 0.01$, significant at the 99% confidence level). In the context of FWI analysis, the direction and magnitude of Z-values obtained from the SK test provide valuable insight into long-term trends in fire danger. Positive Z-values are interpreted as statistically significant increases in fire weather severity over time, suggesting a growing potential for wildfire occurrence and intensity. Conversely, negative Z-values indicate a decreasing trend in fire danger, which may reflect changing meteorological conditions such as increased humidity, reduced temperatures, or higher precipitation. This trend detection framework allows for the identification of both emerging and persistent changes in fire risk across different climate scenarios. For methodological grounding and validation of the SK test application, reference is made to the foundational work by Hirsch and Slack (1984) and its recent implementation in climate-related studies such as Di Nunno et al. (2023).

3. Results

3.1. Historical vs. Future duration/frequency results by FWI class

The data presented in Table 1 offers a detailed evaluation of the evolution of fire danger conditions as represented by the FWI under both historical and projected future climate scenarios.

During the historical baseline period (Figs. 2 and 3), the fire danger landscape is characterized by a predominance of very low fire risk. This category shows a markedly high average duration of approximately 36 months, along with a frequency of 52.14%, indicating that more than half of the time, particularly in central and northern Europe, the region experienced weather conditions associated with minimal fire danger. In contrast, the higher danger classes, including high, very high, and extreme, exhibit significantly shorter durations and lower frequencies. Among these, the extreme category shows a duration of 3.10 months and a frequency of 13.44%, suggesting that while relatively infrequent, extreme fire weather conditions are nonetheless recurrent and not negligible, in particular in Northern Africa.

Under future climate scenarios, a clear shift emerges in both the persistence and occurrence of various fire danger levels, particularly as greenhouse gas concentrations increase. In the moderate-emission RCP4.5 scenario (Supplementary Data Figs. S1–S10), all GCM projections indicate a substantial reduction in the duration of very low FWI conditions, with values ranging from 23.55 (IPSL-CM5A-MR) to 25.16 months (MPI-ESM-LR). This reduction signals a significant contraction in the temporal extent of low-risk periods. Simultaneously, the duration of extreme fire danger increases in all models, reaching values as high as 4.88 months (MPI-ESM-LR). The frequency of extreme FWI conditions under RCP4.5 shows modest increases compared to the historical period, with values fluctuating between 13.51% (EC-EARTH) and 14.31% (MPI-ESM-LR). Although these increases may appear slightly in percentage terms, they are critical when considered in conjunction with the rising duration, indicating not only more frequent extreme fire weather events but also events that persist for longer periods.

More dramatic changes are observed under the high-emission RCP8.5 scenario, which represents a future with limited climate mitigation (Supplementary Data Figs. S11–S20). The average duration of very low FWI conditions continues to decline across all models, reaching a minimum of 23.05 months (HadGEM2-ES), while the durations associated with higher danger classes continue to rise. Particularly noteworthy is the extreme category, which under this scenario shows substantial increases in duration, peaking at 6.38 months according to MPI-ESM-LR, followed by 5.57 months projected by IPSL-CM5A-MR. This pattern indicates a near doubling of the temporal extent of extreme fire weather conditions relative to the historical average. Concurrently, the frequency of extreme fire danger also increases, reaching a maximum of 14.42% (MPI-ESM-LR). This trend reflects not just a growth in the number of months experiencing extreme fire risk, but also an increase in the persistence of these conditions throughout the year.

In parallel, moderate and high FWI categories also show increasing durations and frequencies under future climate scenarios. These rises are especially pronounced under RCP8.5, where some models project durations exceeding three months and frequencies nearing or surpassing 9% for the high category. Although the frequency of very high FWI conditions remains lower than other categories, it still exhibits consistent growth across models and scenarios, indicating a broadening of the fire danger spectrum across all classes, rather than a change confined to the extremes.

Overall, the results suggest a pronounced transformation in the fire weather regime driven by climate change. The decreasing duration of very low fire danger periods, coupled with the increasing persistence and recurrence of high to extreme FWI conditions, portrays a fire-prone future. This transition implies not only more frequent and severe fire weather but also more prolonged episodes that could strain firefighting resources and heighten the risk of large, uncontrollable wildfires. The multi-model ensemble used in this study strengthens the robustness of these projections, providing a comprehensive understanding of potential fire weather evolution under differing climate futures. This assessment underscores the urgency of integrating fire danger projections into climate adaptation and land management strategies to mitigate the rising risks associated with fire in a warming world.

What remains mostly unchanged from the historical period to future projections under both RCP4.5 and RCP8.5 scenarios is the overall spatial pattern of fire danger. Central and Northern Europe consistently exhibit the highest durations and frequencies of very low and low FWI values, reflecting their cooler and more humid climates that continue to suppress fire potential (Galizia et al., 2022). Southern Europe remains a transitional zone, dominated by moderate and high FWI classes, due to its warmer, drier summers and greater sensitivity to climatic shifts (Hetzer et al.,

Table 1
Mean durations and frequencies, calculated across all grid cells, are presented by FWI class for both historical data and GCM projections under the RCP4.5 and RCP8.5 scenarios. The color-bar, for each class, transitions from blue (representing low values) through white (intermediate values) to red (high values).

Duration (months)		Very low	Low	Moderate	High	Very high	Extreme
Historical		35.99	3.39	2.73	2.25	1.37	3.10
RCP4.5	CNRM-CM5	24.55	3.88	3.20	2.75	1.64	4.03
	EC-EARTH	24.22	3.94	3.25	2.97	1.83	3.77
	HadGEM2-ES	24.03	3.72	3.23	2.88	1.61	4.16
	IPSL-CM5A-MR	23.55	3.77	3.17	2.88	1.82	4.25
	MPI-ESM-LR	25.16	3.79	3.08	2.77	1.80	4.88
RCP8.5	CNRM-CM5	24.06	3.93	3.25	2.73	1.65	4.00
	EC-EARTH	24.57	3.89	3.32	3.23	1.95	4.70
	HadGEM2-ES	23.05	3.72	3.25	2.99	1.80	4.83
	IPSL-CM5A-MR	25.36	3.79	3.10	3.09	2.03	5.57
	MPI-ESM-LR	25.02	3.82	3.21	3.06	2.08	6.38
Frequency (%)		Very low	Low	Moderate	High	Very high	Extreme
Historical		52.14	13.13	8.15	7.69	5.46	13.44
RCP4.5	CNRM-CM5	51.31	13.69	7.93	7.73	5.65	13.70
	EC-EARTH	50.02	13.83	8.49	8.32	5.82	13.51
	HadGEM2-ES	50.74	12.91	8.56	8.15	5.77	13.87
	IPSL-CM5A-MR	49.70	13.26	8.61	8.72	6.16	13.55
	MPI-ESM-LR	51.03	13.46	7.75	7.70	5.74	14.31
RCP8.5	CNRM-CM5	51.03	13.73	8.03	7.72	5.64	13.86
	EC-EARTH	49.59	13.50	8.47	8.76	5.78	13.90
	HadGEM2-ES	49.30	13.12	8.83	8.66	5.88	14.21
	IPSL-CM5A-MR	49.38	13.01	8.23	9.09	6.34	13.95
	MPI-ESM-LR	50.42	13.24	7.97	8.02	5.93	14.42

2024). North Africa stands out as the region with the most persistent and frequent occurrences of very high and extreme FWI conditions, both historically and in future projections. Its arid climate and high baseline temperatures make it inherently fire-prone, with climate change further intensifying fire danger levels (Mosha et al., 2025).

This spatial stability highlights the enduring influence of regional climatic and ecological characteristics, even as overall fire danger increases. It underscores the need for region-specific fire management strategies: prevention and monitoring in Central and Northern Europe, adaptation and preparedness in Southern Europe, and more intensive mitigation efforts in North Africa.

3.2. Statistical agreement between historical and GCMs time series

Fig. 4 presents the spatial distribution of the *r* and RMSE values for the overlapping historical period across all GCMs and RCP scenarios. These metrics were calculated to evaluate the consistency between observed data and modeled outputs from the GCMs under both RCP 4.5 and RCP 8.5 scenarios.

Overall, higher correlation values (*r* between 0.8 and 1.0) were observed across extensive areas of Southern Europe and parts of Northern Africa during the overlapping historical period, considering all GCMs and both RCP scenarios for the FWI. These regions include southern Portugal, large portions of Spain and Italy in Western Europe, and most of Greece and Turkey in the Eastern Mediterranean. Notably, similarly high correlations were found in the Mediterranean and inland regions of Algeria. These strong correlations indicate that, across these areas, the GCMs were able to replicate the temporal variability of the FWI reasonably well. This suggests a good agreement between modeled and observed seasonal patterns, particularly regarding the atmospheric drivers of fire weather, such as temperature, wind speed, relative humidity, and precipitation deficits. The Mediterranean basin, known for its pronounced seasonality and relatively stable synoptic climate regimes (e.g., dry, hot summers and mild, wetter winters), likely enhances the models' ability to capture key FWI fluctuations over time.

However, a distinct latitudinal gradient is apparent when moving northward into Central and Northern Europe, where the correlation values tend to decrease. In these regions, *r* values typically range between 0.4 and 0.6, with a further decline to 0.2–0.4 in topographically complex areas such as the Alpine region. This weakening of correlation points to a reduced capacity of GCMs to reproduce the interannual and seasonal dynamics of the FWI in these zones. Several factors can explain this discrepancy. First, the FWI is particularly sensitive to fine-scale interactions between multiple meteorological variables. In Central and Northern Europe, where climatic conditions are more variable and less dominated by stable seasonal patterns, capturing the co-variability of fire weather drivers becomes more challenging. Second, mountainous regions like the Alps present well-known difficulties for coarse-

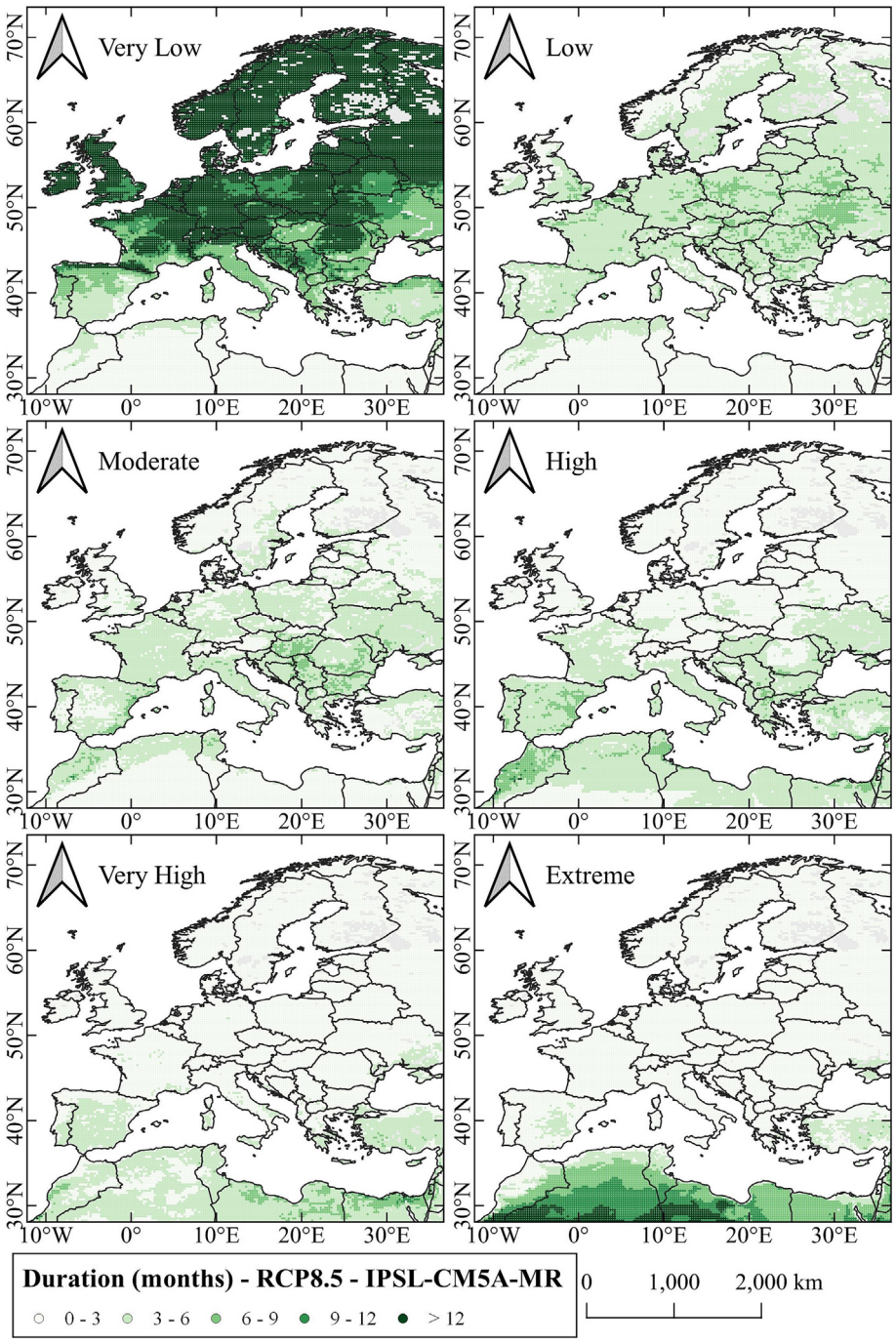

Fig. 2. Historical durations by FWI class.

resolution GCMs due to their sharp elevation gradients, localized weather systems, and microclimatic effects. These features are typically underrepresented in GCM outputs, leading to smoothed simulations that fail to capture the nuanced variability in FWI-related conditions. This results in weaker correlations even if the broad-scale climate trends are reasonably approximated.

Interestingly, RMSE reveals an inverse spatial pattern compared to the correlation coefficient. The lowest RMSE values, indicating smaller average deviations between historical and GCM-simulated FWI, are observed in Northern Europe, including the Alps, Scandinavia, the Baltic states, and the UK. In contrast, Northern Africa has the highest RMSE values, consistent with its high FWI means and variability due to intense fire weather conditions (see also Fig. 1). This contrast highlights the different statistical roles of *r* and RMSE. While *r* captures how well models reproduce temporal variability, RMSE reflects the absolute magnitude of errors. In regions like the Alps or Northern Europe, where FWI values are generally low and stable, GCMs may have approximate mean conditions well, resulting in low RMSE despite weaker correlations due to limited variability or unresolved local dynamics. Conversely, in fire-prone areas such as Northern Africa and the Mediterranean, high *r* values indicate that models track temporal patterns reasonably well, but large RMSE values suggest systematic biases in key variables (e.g., temperature, precipitation), which translate into significant absolute errors. The higher FWI magnitude and variability in these regions amplify such discrepancies.

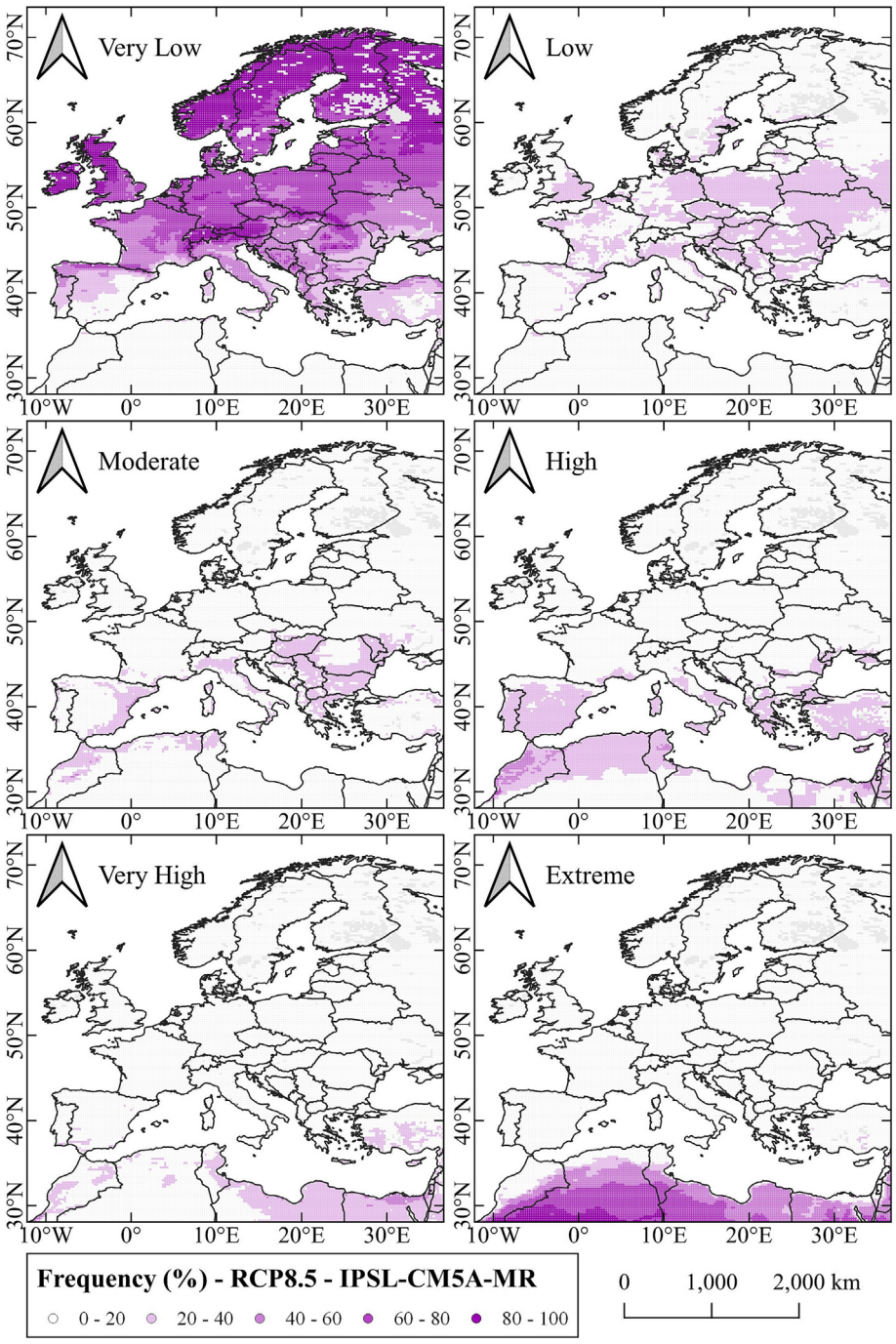

Fig. 3. Historical frequencies by FWI class.

This divergence between *r* and RMSE underlines the need to evaluate both metrics together, especially for indices like the FWI that are strongly influenced by latitude and regional climate characteristics.

In addition, the combined box and violin plot for all metrics were given in Fig. 5, offering a comparative view of central tendencies and variability in model performance, reflecting both the accuracy and consistency of simulated FWI values.

WI values were consistently high, with HadGEM2-ES under both scenarios showing particularly strong agreement (mean WI = 0.796 for RCP8.5). This suggests that these models not only captured the temporal variability of FWI but also reproduced its intensity with high fidelity. Slightly lower WI values observed for EC-EARTH (mean WI = 0.778 for RCP8.5) imply that while it reproduced trends reasonably well, there may be modest discrepancies in the amplitude of extremes or transitions.

Models with higher WI typically also showed elevated KGE values, reinforcing the reliability of their projections. HadGEM2-ES once again emerged as one of the top-performing models (mean KGE = 0.636 for RCP8.5), with KGE values reflecting balanced performance across all components. Conversely, models with lower KGE, such as EC-EARTH (mean KGE = 0.608 for RCP4.5), tended to exhibit deviations in either bias or variability despite acceptable correlation, indicating a less robust replication of observed FWI patterns.

Across most models, MAE values remained within an acceptable range, with slight increases under the RCP8.5 scenario (between

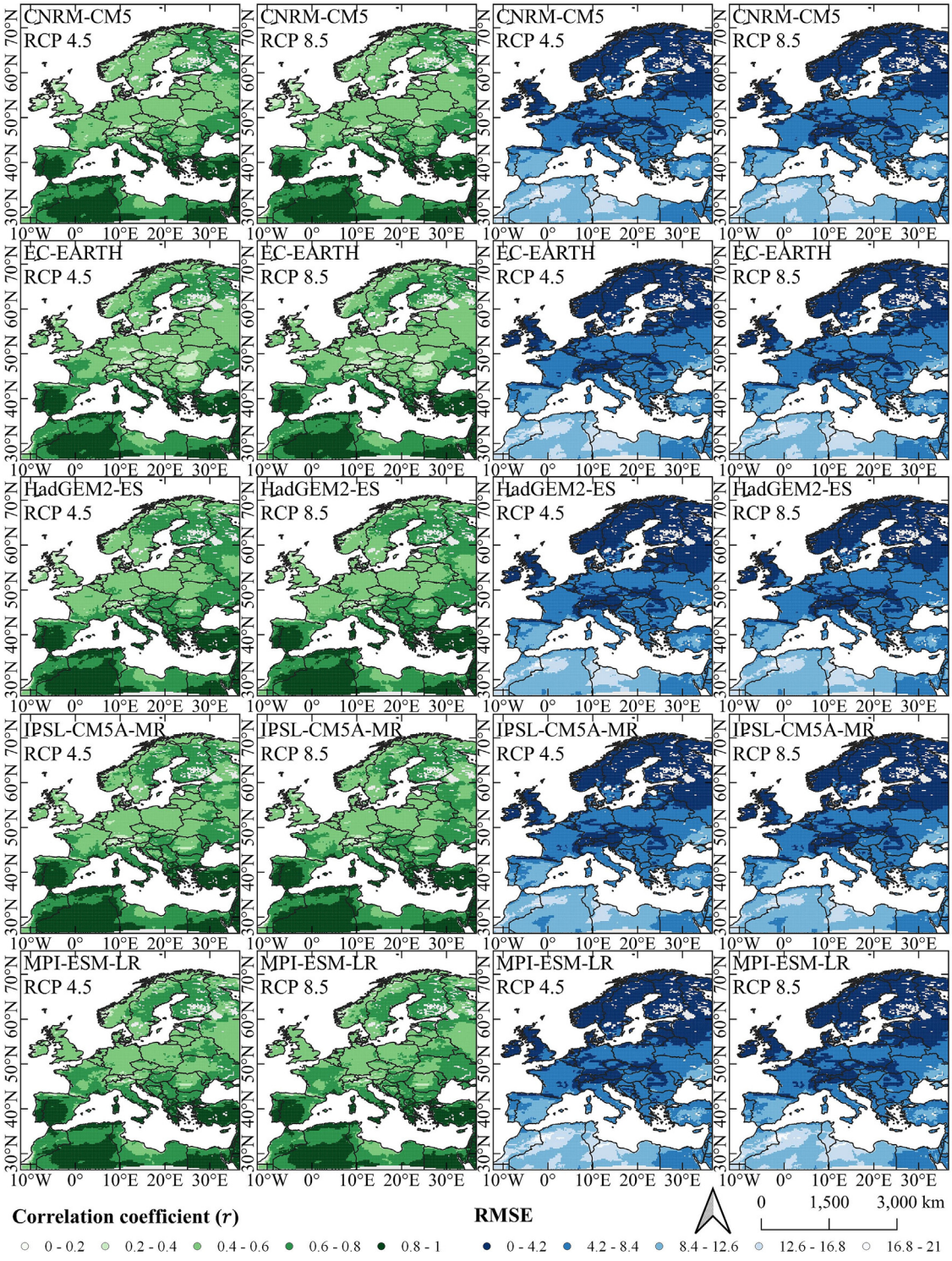

Fig. 4. Spatial distribution of the correlation coefficient (r) and Root Mean Square Error (RMSE) computed between historical and Global Climate Models (GCMs) time series for the overlapping historical period under Representative Concentration Pathways (RCP) 4.5 and 8.5. The five GCMs belong to the Coupled Model Intercomparison Project Phase 5 (CMIP5): Centre National de Recherches Météorologiques – Coupled Model version 5 (CNRM-CM5, developed by CNRM-CERFACS, France), European Consortium Earth System Model (EC-EARTH, developed by the Irish Centre for High-End Computing, ICHEC, Ireland), Institut Pierre-Simon Laplace – Coupled Model version 5A, Medium Resolution (IPSL-CM5A-MR, developed by IPSL, France), Hadley Centre Global Environment Model version 2 – Earth System (HadGEM2-ES, developed by the UK Met Office, United Kingdom), and Max Planck Institute Earth System Model, Low Resolution (MPI-ESM-LR, developed by the Max Planck Institute for Meteorology, Germany).

4.180 for IPSL-CM5A-MR and 4.461 for EC-EARTH), potentially reflecting heightened variability in projected fire weather conditions. The normalized RAE metric revealed greater differentiation among the models. Notably, the RAE value for IPSL-CM5A-MR under RCP8.5, equal to 0.630, was the lowest, suggesting particularly strong relative accuracy during this more extreme scenario, while EC-EARTH showed the highest value, equal to 0.669, under RCP4.5.

Collectively, the combined box and violin plots underscore the generally high degree of agreement between observed and simu-

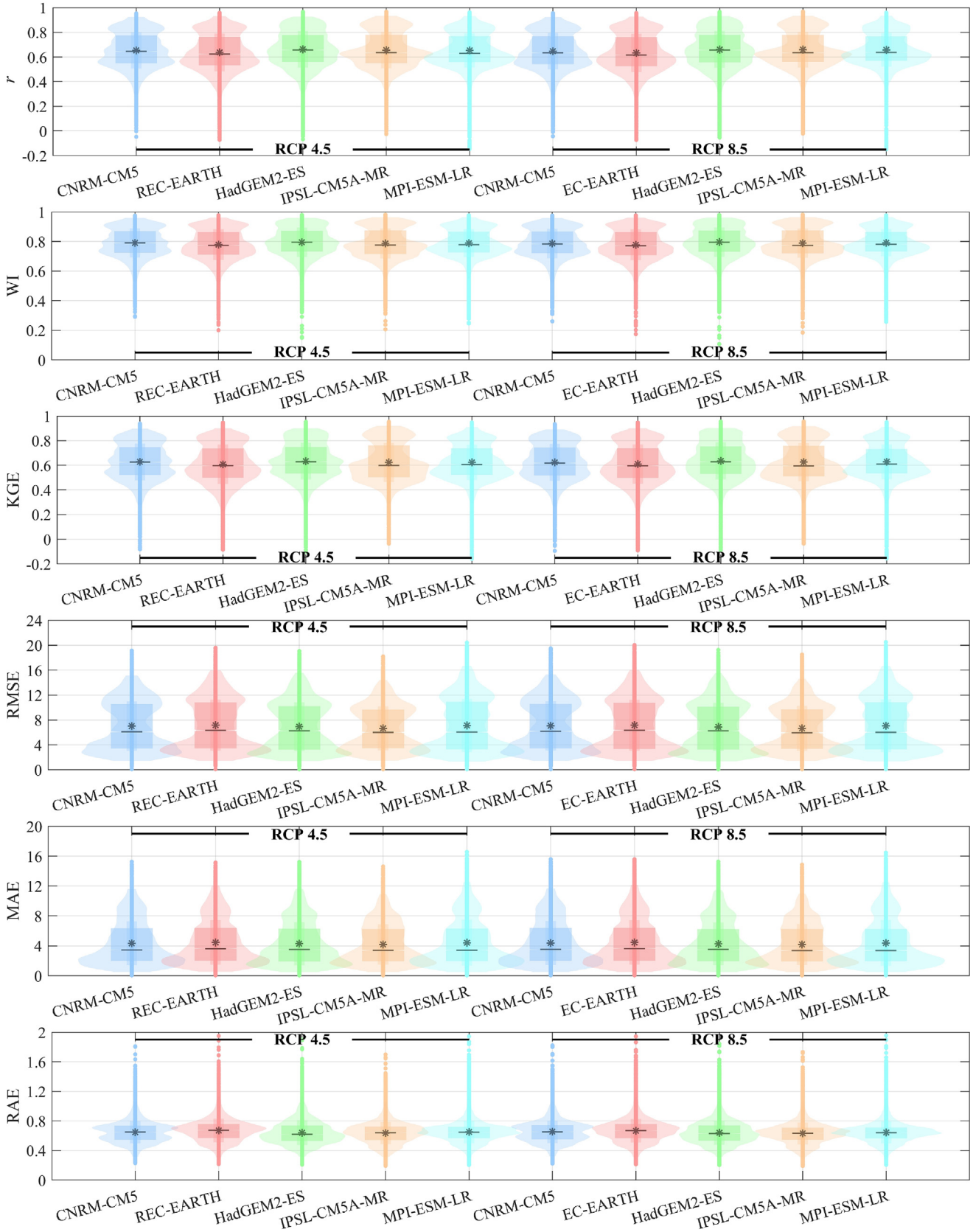

Fig. 5. Combined box and violin plots for the different performance metrics: correlation coefficient (*r*), Willmott Index (WI), Kling–Gupta Efficiency (KGE), Root Mean Square Error (RMSE), Mean Absolute Error (MAE) and Relative Absolute Error (RAE).

lated FWI. These results strengthen the credibility of using multi-model ensembles for projecting future fire weather risk, while also informing model selection and weighting in impact assessments.

3.3. Trend analysis

The SK test was applied to analyze FWI trends across the study areas, revealing both increasing and decreasing patterns (Fig. 6).

Historical data showed *Z*-values greater than 2.576, indicating statistically significant increasing trends at the 99% confidence level, across most of Europe and North Africa, suggesting a growing potential for wildfire occurrence and intensity. In contrast, northern Europe, including England, the Scandinavian countries, and Italy, exhibited *Z*-values between −1.96 and 1.96, indicating no statistically significant trends.

Turning to the GCM projections, CNRM-CM5 under the RCP4.5 scenario showed *Z*-values greater than 2.576 only in limited areas, including southern Turkey, Morocco, and the Alpine region of Italy. Most of Europe displayed negative *Z*-values, with some regions, such as the Swedish coast along the Baltic Sea and northern Germany, showing statistically significant decreasing trends at the 95% confidence level (*Z*-values between −1.96 and −2.576). Under the RCP8.5 scenario, however, the model projected *Z*-values above 2.576 across much of southern Europe and northern Africa, indicating widespread significant increases in FWI trends. Eastern European countries, including Hungary and Ukraine, also exhibited *Z*-values above 2.576. Conversely, Scandinavian countries showed less pronounced trends, with some areas between Sweden and Finland displaying statistically significant negative *Z*-values, decreasing trend in fire danger, which may reflect changing meteorological conditions such as increased humidity, reduced temperatures.

EC-EARTH under RCP4.5 showed *Z*-values greater than 2.576 in Morocco (consistent with CNRM-CM5) and in the eastern Mediterranean, including Greece and Turkey. Most of Europe exhibited no statistically significant trends, although some regions in Norway and Ireland displayed statistically significant decreasing trends. Under RCP8.5, the patterns were more pronounced than those projected by CNRM-CM5, with nearly the entire study area, except the Scandinavian countries and parts of the UK, showing *Z*-values greater than 2.576, indicating widespread increasing trends.

HadGEM2-ES under RCP4.5 projected *Z*-values greater than 2.576 across much of southern Europe, extending into central European countries such as France, the Netherlands, and most of Germany. In northern Africa, Algeria, Tunisia, and parts of Egypt also exhibited strong increasing trends. Under RCP8.5, projections were broadly consistent with the other GCMs, with nearly all of North Africa and most European countries showing statistically significant increases. The Scandinavian countries, along with

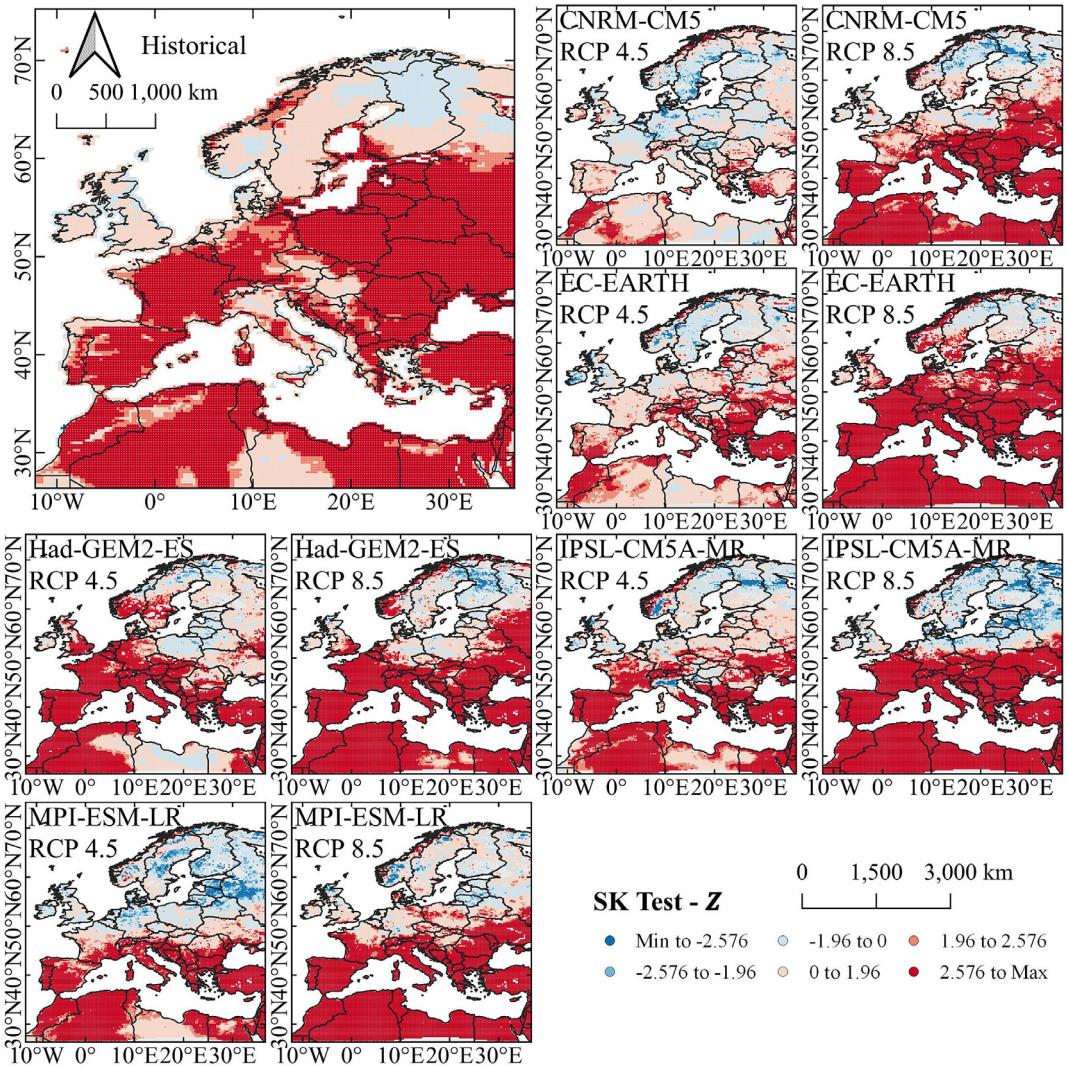

Fig. 6. *Z* parameter of the SK test.

Poland and the UK, generally showed no statistically significant trends, although northern Sweden and Finland displayed significant decreasing trends, echoing patterns observed in CNRM-CM5.

IPSL-CM5A-MR under RCP4.5 indicated Z-values greater than 2.576 in northern Africa (Morocco, Algeria, Tunisia, and Egypt) and in the Mediterranean region, while northern Italy, particularly the Po Basin, exhibited marked negative trends. Under RCP8.5, a stronger latitudinal gradient was observed compared to other GCMs, with statistically significant positive trends in all countries south of Germany and Poland, and no significant trends, positive or negative, in northern Europe.

MPI-ESM-LR under RCP4.5 projected pronounced increasing trends across all of southern Europe and northern Africa, while northern Europe, especially the Baltic countries, showed negative trends. Under RCP8.5, positive trends became even more pronounced across the southern regions. The Baltic countries continued to exhibit negative trends, although these were no longer statistically significant.

Fig. 7 illustrates box plots of Z-values for the FWI, categorized by macro-regions: North Africa (< 36°N), Southern Europe (36°N – 42°N), Central Europe (42°N – 50°N), and Northern Europe (≥ 50°N). In addition, the box plots display dashed lines corresponding to $Z = \pm 1.96$ (indicating statistically significant trends at $p \leq 0.05$) and solid lines corresponding to $Z = \pm 2.576$ (indicating statistically significant trends at $p \leq 0.01$).

In the historical period, all macro-regions show positive Z-values, suggesting increasing trends in FWI. Central Europe stands out, as both the 25th and 75th percentiles exceed the critical threshold of $Z = 1.96$, indicating a statistically significant upward trend. This suggests that fire weather conditions in central Europe have already intensified in recent decades, likely reflecting broader climate warming signals.

Looking ahead to projections under the RCP4.5 scenario, the models CNRM-CM5 and EC-EARTH generally produce positive Z-values, though most remain within the ±1.96 range, implying trends that are not statistically significant. However, EC-EARTH shows a stronger signal in southern Europe, where the upper bounds of the interquartile range exceed $Z = 1.96$, suggesting a moderately significant increase in FWI. Moreover, IPSL-CM5A-MR and MPI-ESM-LR projects a robust and significant rise in FWI across southern Europe, with the entire interquartile range exceeding $Z = 2.576$ ($p \leq 0.01$), highlighting a particularly strong future fire risk in this region. On the other hand, MPI-ESM-LR reveals a nearly negative distribution for northern Europe, with the lower quartile approaching $Z = -1.96$, suggesting the possibility of a slight but statistically significant decline in FWI for that region.

Under the more extreme RCP8.5 scenario, the projections become more pronounced. Except for northern Europe, which remains close to neutral or slightly positive depending on the model, all other regions exhibit strongly significant upward trends. The Z-values in central and southern Europe, and also in northern Africa, especially under IPSL-CM5A-MR, are particularly striking, with mean values nearing 10 and all interquartile ranges well above $Z = 2.576$. This signals a high confidence in severe increases in fire weather conditions under continued high-emissions pathways. Northern Europe remains an outlier, where IPSL-CM5A-MR again projects a lower quartile close to $Z = -1.96$, indicating a potential, but weak, negative trend.

Altogether, these results reflect a clear spatial and scenario-based differentiation in FWI trends. While past increases are already evident, future projections, especially under RCP8.5, suggest that central and southern Europe could face significantly heightened fire weather risks, underscoring the urgency of regional adaptation strategies.

4. Discussion

4.1. Consistency and divergence among GCMs and RCPs

The use of multiple GCMs and two distinct RCP scenarios in this study enables a broader interpretation of potential fire weather trajectories, while also highlighting areas of model convergence and divergence that are critical for climate impact assessment. While ensemble means provide a general picture of future fire danger intensification, the spread among individual models reveals key sources of uncertainty that merit closer examination.

Agreement between historical and GCMs data, for the overlapping period is generally stronger in regions with pronounced seasonality and relatively stable synoptic patterns, such as southern Europe and North Africa, where fire weather is closely tied to persistent climatic drivers. In these areas, the structure of the climate system is sufficiently captured by the coarse resolution of GCMs, leading to consistent projections across models. Conversely, divergence is more evident in regions with higher climatic variability, complex topography, or transitional climate regimes, where local dynamics play a disproportionate role. These include central and northern Europe, as well as mountainous zones, where model outputs are less coherent and sometimes even contradictory in terms of trend direction or magnitude.

The discrepancies across GCMs stem not only from differences in spatial resolution and physical parameterizations, but also from their sensitivity to feedback mechanisms such as soil moisture-atmosphere coupling or vegetation responses, factors that are highly relevant to fire weather dynamics yet are modeled with varying degrees of sophistication (Colmet-Daage et al., 2018). Additionally, each model's historical performance in reproducing key fire-weather-related variables (e.g., temperature extremes, precipitation deficits, wind patterns) can influence its future projections, thereby introducing structural biases (Achugbu et al., 2025).

RCP-related differences further illustrate the compounding influence of emissions pathways on fire danger evolution. While RCP4.5 and RCP8.5 often display qualitatively similar trends, their quantitative differences are nontrivial (Rovithakis et al., 2022). These gaps underscore the sensitivity of fire danger indices like the FWI to incremental warming, especially when thresholds for high and extreme fire danger are surpassed more frequently and for longer durations. Such outcomes reinforce the importance of scenario-based planning in fire management, where even moderate mitigation efforts can meaningfully alter long-term fire risk.

Finally, the observed divergence among GCMs should not be viewed solely as a limitation but as a reflection of the real uncertainty embedded in future climate conditions. Rather than seeking deterministic projections, fire risk assessments should leverage this spread to define plausible bounds for adaptation strategies. In this context, the ensemble approach adopted here serves not only to average out extremes but also to expose the range of possibilities that stakeholders must prepare for under a changing climate.

4.2. Implications for fire seasonality and risk management

The projected shifts in fire weather conditions across Europe and North Africa carry significant implications for the seasonality of wildfire risk and the corresponding adaptation strategies (El Garroussi et al., 2024). As climate change alters the temporal structure of fire-prone periods, the traditional boundaries of fire seasons may become increasingly blurred, necessitating a re-evaluation of preparedness timelines and operational protocols.

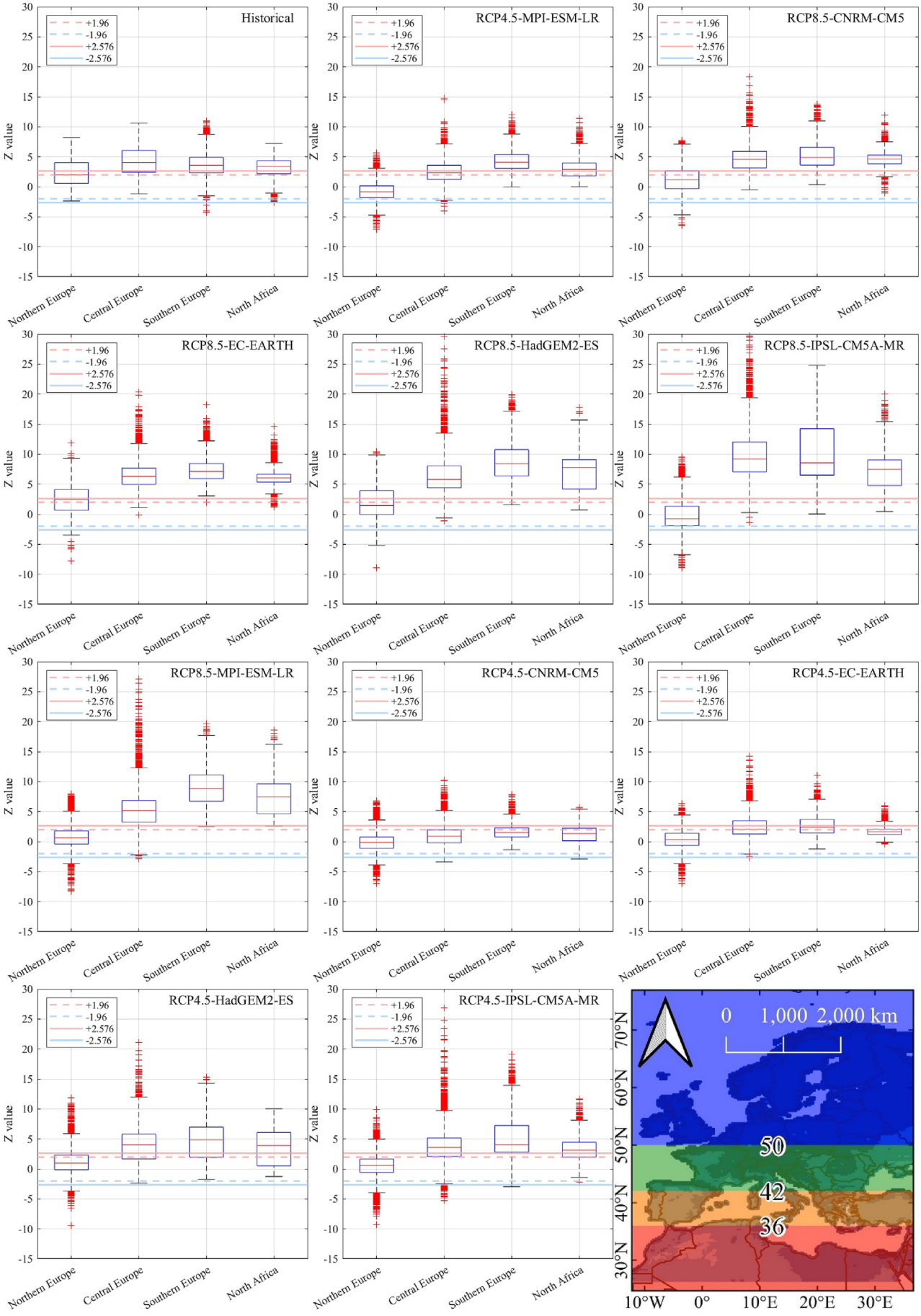

Fig. 7. Box plots of *Z* values. On the bottom right, an outline map with the macro-regions.

One of the most salient findings is the projected extension of high and extreme fire weather conditions into months that were historically characterized by lower fire danger. This temporal expansion of the fire season, more pronounced under high-emission scenarios, suggests that fire management systems will need to shift from seasonal readiness toward a more continuous state of alert. In regions such as southern Europe and the Mediterranean basin, where fire seasons have historically been concentrated in the summer months, earlier onsets and delayed terminations could lead to longer periods of sustained pressure on firefighting infrastructure and personnel.

Moreover, changes in fire danger frequency and persistence may outpace existing institutional and logistical capacities. Increased duration of extreme fire weather not only raises the probability of ignition and spread but also reduces recovery windows between fire events. This scenario places a premium on adaptive risk management approaches that are both flexible and anticipatory. For example, fire prevention efforts may need to be implemented earlier in the year, while resource allocation, including aerial assets, personnel, and funding, must account for the higher likelihood of multi-peak fire seasons.

From a planning perspective, spatial disparities in projected fire danger trends also call for differentiated regional responses. While North Africa and southern Europe are expected to face more frequent and intense fire events, some parts of northern and central Europe, currently perceived as low-risk, may experience a relative increase in fire susceptibility (Miller et al., 2024). This emerging vulnerability necessitates the expansion of fire awareness campaigns, training programs, and resource distribution in areas not traditionally prioritized for fire risk.

Furthermore, the increasing uncertainty surrounding fire season dynamics underscores the need to integrate fire weather projections into long-term land use and forest management policies (Dupuy et al., 2020). This includes revisiting prescribed burning schedules, adjusting forest thinning practices, and reassessing zoning regulations in fire-prone areas. Proactive strategies that anticipate shifting fire regimes can reduce future exposure and enhance ecosystem resilience.

Overall, the evolving fire seasonality patterns revealed by this study challenge the adequacy of static fire management frameworks. As climatic conditions continue to drive longer, more intense, and less predictable fire seasons, fire governance must become more dynamic, anchored in climate-informed decision-making and supported by robust early warning systems tailored to new seasonal norms.

4.3. Uncertainties related to model spread and data processing

Despite the robustness provided by a multi-model and multi-scenario framework, this study, like all climate impact assessments, carries inherent uncertainties stemming from both model variability and methodological choices. Understanding and acknowledging these uncertainties is essential for interpreting the results and translating them into actionable risk management strategies.

A key source of uncertainty lies in the spread among GCMs. While general trends, such as the increase in high and extreme fire danger, are broadly consistent, the magnitude, spatial distribution, and even sign of trends can vary notably between models. This variation reflects structural differences in how each GCM represents atmospheric dynamics, land–atmosphere interactions, and climate feedback mechanisms (Gallo et al., 2023). For instance, differences in how precipitation variability, evapotranspiration, and soil moisture are simulated can substantially affect the resulting FWI values, particularly in transitional or topographically complex regions. These structural disparities underscore the importance of interpreting ensemble outputs not as definitive forecasts, but as probabilistic envelopes of plausible futures.

Another layer of uncertainty is introduced by the choice of emission scenarios. While RCP4.5 and RCP8.5 represent well-established pathways, real-world emissions may evolve along trajectories that fall between or outside these bounds. Moreover, downscaling assumptions and the absence of dynamic vegetation modeling further limit the representation of feedbacks that may become increasingly important in future fire regimes, such as land cover shifts, fuel load changes, and anthropogenic modifications of the landscape.

Data processing decisions also contribute to uncertainty. In the present study, the FWI was obtained as a pre-calculated monthly variable from the Copernicus Climate Data Store, derived from both the ERA5 reanalysis and GCM projections. The use of monthly averaged FWI values, while facilitating consistent and scalable long-term trend analysis across large domains, inevitably smooths out short-term variability and may underestimate extreme fire weather peaks that occur on daily or weekly scales (Di Giuseppe et al., 2025). Similarly, the reliance on a single reanalysis product (ERA5) for the historical baseline, although among the most comprehensive and reliable, may still embed biases related to input observations and assimilation methods. Such biases can propagate through the comparison with GCM outputs, affecting correlation metrics and trend assessments.

In addition, the spatial resolution of both the historical (ERA5) and projected (GCM-based) FWI datasets, provided at a consistent scale through the Copernicus Climate Data Store, is appropriate for continental-scale analysis. However, this resolution may still obscure localized fire-weather dynamics that are critical for operational fire management. This limitation is particularly relevant in heterogeneous landscapes, where microclimatic variability and land use heterogeneity can drive significant deviations from regional fire weather trends (Jain et al., 2020).

Finally, the application of the SK test, while robust to non-normal distributions and seasonality, does not account for non-linear or abrupt changes in fire weather behavior. Complementary techniques, such as Bayesian Estimator of Abrupt change, Seasonality, and Trend (BEAST), could offer additional insights into potential regime shifts or threshold behaviors under climate change (Di Nunno et al., 2024; Di Nunno and Granata, 2025).

Taken together, these uncertainties do not undermine the overall conclusions of the study but rather emphasize the need for careful interpretation and cautious extrapolation. Future research should aim to refine projections through higher-resolution modeling, improved representation of vegetation-fire-climate interactions, and ensemble approaches that integrate a broader range of climate scenarios and data sources.

4.4. Comparison with other regional studies

Projections of increasing fire danger under climate change are consistent with a growing body of regional research across Europe and North Africa. Numerous studies report significant increases in FWI values and related wildfire risks under various greenhouse gas emission scenarios. The present findings broadly align with these projections, while offering additional spatial continuity and model diversity across the European–North African domain.

In southeastern France, Varela et al. (2019) simulated future fire behavior using the Minimum Travel Time algorithm and identified trends toward larger wildfires, increased burn probability, and higher fire-line intensities. These projections, which focus on fire behavior metrics at a regional scale, are consistent with broader trends observed here in terms of increased frequency and duration of high and extreme FWI values.

Dupuy et al. (2020) reviewed 23 studies on future fire danger in southern Europe and reported increases in both danger levels and burned area, with fire-prone regions projected to expand northward and into higher elevations. Similar patterns of latitudinal and altitudinal expansion are reflected in the present results, particularly under the RCP8.5 scenario, which shows significant increases in fire danger across southern and central Europe.

Aparício et al. (2022), examining the Transboundary Biosphere Reserve of Meseta Ibérica, projected a threefold increase in the annual number of extreme fire danger days by the end of the century. Their findings are in line with results observed in southwestern Europe, where a consistent increase in extreme FWI conditions is projected across all models and scenarios evaluated in this study.

In Greece, Rovithakis et al. (2022) reported up to 40 additional high fire danger days annually under RCP8.5, with pronounced changes in the southern and eastern parts of the country. Similar increases are identified across southeastern Europe in the current analysis, particularly in Crete, Attica, and the Peloponnese, where model consensus indicates a significant intensification of fire danger conditions over time.

Tomašević et al. (2022) highlighted a northward and inland expansion of fire risk in Croatia, along with an earlier onset and later end to the fire season. These findings are consistent with the general extension of fire danger periods observed in the current dataset, especially across central and eastern Europe, where increasing durations in high FWI categories suggest prolonged seasonal exposure.

Studies from central Europe also indicate rising fire danger. Leonardos et al. (2024) and Miller et al. (2024) identified increasing severity and duration of fire seasons in temperate regions, challenging historical assumptions about low fire risk in these areas. The present results show similar spatial patterns, with elevated moderate and high FWI values projected across central and northern Europe, particularly under RCP8.5.

Taken together, these regional studies provide strong support for the trends identified in the current assessment. While methods and geographic areas of focus differ, there is consistent evidence across the literature of increasing fire danger in response to climate change. The present analysis builds on this foundation by applying a standardized classification of fire danger across a broader spatial domain and using a multi-model, multi-scenario framework to ensure robustness and comparability. This integrated approach enables the detection of both regional consistencies and cross-boundary variations in fire weather trends, supporting the development of more geographically inclusive and forward-looking fire risk management strategies.

5. Conclusion

This study assessed historical and projected trends in fire weather conditions across Europe and North Africa using the FWI, supported by both reanalysis data and climate projections from five GCMs under RCP4.5 and RCP8.5 scenarios.

The analysis highlighted clear spatiotemporal patterns in fire danger evolution, revealing a systematic decline in very low fire danger periods and a corresponding increase in the duration and frequency of high and extreme FWI categories. These changes are particularly pronounced under the high-emission RCP8.5 scenario, with southern Europe and northern Africa emerging as hot-spots of future fire risk.

The findings underscore the growing urgency for integrating climate-informed fire risk assessments into national and regional fire management strategies. In particular, the projected lengthening and intensification of fire seasons suggest the need to revise preparedness protocols, resource allocation, and land-use planning frameworks. Firefighting systems will increasingly need to operate beyond traditional seasonal boundaries, while new areas, particularly in temperate zones, may require the establishment or expansion of fire risk monitoring and mitigation infrastructure. Adaptation efforts should also account for the compound effects of changing climate, vegetation, and land use on fire behavior and exposure.

Future research should address key limitations of this study to improve fire danger projections. The reliance on monthly FWI may underestimate short-term extremes, and the coarse spatial resolution of GCM outputs limits the ability to capture localized fire dynamics, particularly in complex terrain. Additionally, using only two emission scenarios and a limited number of models restricts the exploration of projection uncertainties. The absence of dynamic vegetation and socio-economic factors further narrows the scope. Moreover, treating the future projection period as a single continuous epoch may overlook possible intra-period trends, especially in light of global climate targets set for mid-century (e.g., net-zero emissions by 2050). Splitting this period into two sub-epochs (e.g., 2025–2050 and 2051–2098) could provide deeper insight into temporal shifts in fire danger. Incorporating higher-resolution regional simulations, daily or sub-daily fire weather assessments, and integrating socio-economic vulnerability and suppression capacity would enhance the accuracy and practical relevance of future fire risk assessments.

CRediT authorship contribution statement

Fabio Di Nunno: Writing – original draft, Software, Methodology, Investigation, Formal analysis, Data curation, Conceptualization. **Francesco Granata:** Writing – original draft, Visualization, Supervision, Methodology, Investigation, Data curation.

Declaration of competing interest

The authors declare that they have no known competing financial interests or personal relationships that could have appeared to influence the work reported in this paper.

Appendix A. Supplementary data

Supplementary data to this article can be found online at https://doi.org/10.1016/j.gsf.2025.102178.

References

Abatzoglou, J.T., Williams, A.P., 2016. Impact of anthropogenic climate change on wildfire across western US forests. Proc. Natl. Acad. Sci. U.S.A. 113 (42), 11770–11775. https://doi.org/10.1073/pnas.1607171113.

Abatzoglou, J.T., Williams, A.P., Barbero, R., 2019. Global emergence of anthropogenic climate change in fire weather indices. Geophys. Res. Lett. 46 (1), 326–336.

Aparício, B.A., Santos, J.A., Freitas, T.R., Sá, A.C.L., Pereira, J.M.C., Fernandes, P.M., 2022. Unravelling the effect of climate change on fire danger and fire behaviour in the transboundary biosphere reserve of Meseta Ibérica (Portugal-Spain). Clim. Change 173, 5. https://doi.org/10.1007/s10584-022-03399-8.

Achugbu, I.C., Chen, L., Hu, Q., Muñoz-Arriola, F., 2025. Evaluating the historical performance and future change in extreme precipitation indices over the Missouri river basin based on NA-CORDEX multimodel ensemble. Atmosphere 16, 579. https://doi.org/10.3390/atmos16050579.

Avcıoğlu, A., Akbaş, A., Görüm, T., Yetemen, Ö., 2025. The compound effect of topography, weather, and fuel type on the spread and severity of the largest wildfire in NW of Turkey. Nat. Hazards 121, 3219–3237. https://doi.org/10.1007/s11069-024-06885-7.

Bedia, J., Herrera, S., Martín, D.S., Koutsias, N., Gutiérrez, J.M., 2013. Robust projections of fire weather index in the Mediterranean using statistical downscaling. Clim. Change 120, 229–247. https://doi.org/10.1007/s10584-013-0787-3.

Bedia, J., Golding, N., Casanueva, A., Iturbide, M., Buontempo, C., Gutiérrez, J.M., 2018. Seasonal predictions of fire weather index: Paving the way for their

operational applicability in Mediterranean Europe. Clim. Serv. 9, 101–110. https://doi.org/10.1016/j.cliser.2017.04.001.
Berio Fortini, L., Kaiser, L.R., Frazier, A.G., Giambelluca, T.W., 2023. Examining current bias and future projection consistency of globally downscaled climate projections commonly used in climate impact studies. Clim. Change 176, 169. https://doi.org/10.1007/s10584-023-03623-z.
Caesar, J., Palin, E., Liddicoat, S., Lowe, J., Burke, E., Pardaens, A., Sanderson, M., Kahana, R., 2013. Response of the HadGEM2 earth system model to future greenhouse gas emissions pathways to the year 2300. J. Climate 26, 3275–3284. https://doi.org/10.1175/JCLI-D-12-00577.1.
Calheiros, T., Pereira, M.G., Nunes, J.P., 2021. Assessing impacts of future climate change on extreme fire weather and pyro-regions in Iberian Peninsula. Sci. Total Environ. 754, 142233.
Cane, D., Ciccarelli, N., Gottero, F., Francesetti, A., Pelfini, F., Pelosini, R., 2008. Fire weather index application in north-western Italy. Adv. Sci. Res. 2 (1), 77–80.
Carvalho, A.C., Carvalho, A., Martins, H., Marques, C., Rocha, A., Borrego, C., Viegas, D. X., Miranda, A.I., 2011. Fire weather risk assessment under climate change using a dynamical downscaling approach. Environ. Model. Softw. 26 (9), 1123–1133.
Colmet-Daage, A., Sanchez-Gomez, E., Ricci, S., Llovel, C., Estupina, V.B., Quintana-Seguí, P., Llasat, M.C., Servat, E., 2018. Evaluation of uncertainties in mean and extreme precipitation under climate change for northwestern Mediterranean watersheds from high-resolution Med and Euro-CORDEX ensembles. Hydrol. Earth Syst. Sci. 22, 673–687. https://doi.org/10.5194/hess-22-673-2018.
Di Giuseppe, F., McNorton, J., Lombardi, A., Wetterhall, F., 2025. Global data-driven prediction of fire activity. Nat. Commun. 16, 2918. https://doi.org/10.1038/s41467-025-58097-7.
Di Nunno, F., De Matteo, M., Izzo, G., Granata, F., 2023. A combined clustering and trends analysis approach for characterizing reference evapotranspiration in Veneto. Sustainability 15 (14), 11091.
Di Nunno, F., de Marinis, G., Granata, F., 2024. Analysis of SPI index trend variations in the United Kingdom - A cluster-based and Bayesian ensemble algorithms approach. J. Hydrol. Reg. Stud. 52, 101717. https://doi.org/10.1016/j.ejrh.2024.101717.
Di Nunno, F., Granata, F., 2025. Unraveling drought patterns and abrupt changes in the Western Alps: A dual index approach. Earth Syst. Environ. 9, 1253–1272. https://doi.org/10.1007/s41748-025-00633-y.
Döscher, R., Acosta, M., Alessandri, A., Anthoni, P., Arsouze, T., Bergman, T., Bernardello, R., Boussetta, S., Caron, L.-P., Carver, G., Castrillo, M., Catalano, F., Cvijanovic, I., Davini, P., Dekker, E., Doblas-Reyes, F.J., Docquier, D., Echevarria, P., Fladrich, U., Fuentes-Franco, R., Gröger, M., Hardenberg, J., Hieronymus, J., Karami, M.P., Keskinen, J.-P., Koenigk, T., Makkonen, R., Massonnet, F., Ménégoz, M., Miller, P.A., Moreno-Chamarro, E., Nieradzik, L., van Noije, T., Nolan, P., O'Donnell, D., Ollinaho, P., van den Oord, G., Ortega, P., Prims, O.T., Ramos, A., Reerink, T., Rousset, C., Ruprich-Robert, Y., Le Sager, P., Schmith, T., Schrödner, R., Serva, F., Sicardi, V., Sloth Madsen, M., Smith, B., Tian, T., Tourigny, E., Uotila, P., Vancoppenolle, M., Wang, S., Wårlind, D., Willén, U., Wyser, K., Yang, S., Yepes-Arbós, X., Zhang, Q., 2022. The EC-Earth3 earth system model for the coupled model intercomparison project 6. Geosci. Model Dev. 15, 2973–3020. https://doi.org/10.5194/gmd-15-2973-2022.
Dufresne, J.-L., Foujols, M.-A., Denvil, S., Caubel, A., Marti, O., Aumont, O., Balkanski, Y., Bekki, S., Bellenger, H., Benshila, R., Bony, S., Bopp, L., Braconnot, P., Brockmann, P., Cadule, P., Cheruy, F., Codron, F., Cozic, A., Cugnet, D., de Noblet, N., Duvel, J.-P., Ethé, C., Fairhead, L., Fichefet, T., Flavoni, S., Friedlingstein, P., Grandpeix, J.-Y., Guez, L., Guilyardi, E., Hauglustaine, D., Hourdin, F., Idelkadi, A., Ghattas, J., Joussaume, S., Kageyama, M., Krinner, G., Labetoulle, S., Lahellec, A., Lefebvre, M.-P., Lefevre, F., Levy, C., Li, Z.X., Lloyd, J., Lott, F., Madec, G., Mancip, M., Marchand, M., Masson, S., Meurdesoif, Y., Mignot, J., Musat, I., Parouty, S., Polcher, J., Rio, C., Schulz, M., Swingedouw, D., Szopa, S., Talandier, C., Terray, P., Viovy, N., Vuichard, N., 2013. Climate change projections using the IPSL-CM5 Earth System Model: From CMIP3 to CMIP5. Clim. Dyn. 40, 2123–2165. https://doi.org/10.1007/s00382-012-1636-1.
Dupuy, J.-L., Fargeon, H., Martin-StPaul, N., Pimont, F., Ruffault, J., Guijarro, M., Hernando, C., Madrigal, J., Fernandes, P., 2020. Climate change impact on future wildfire danger and activity in southern Europe: A review. Ann. Forest. Sci. 77, 35. https://doi.org/10.1007/s13595-020-00933-5.
El Garroussi, S., Di Giuseppe, F., Barnard, C., Wetterhall, F., 2024. Europe faces up to tenfold increase in extreme fires in a warming climate. Npj Clim. Atmos. Sci. 7, 30. https://doi.org/10.1038/s41612-024-00575-8.
Feron, S., Cordero, R.R., Damiani, A., MacDonell, S., Pizarro, J., Goubanova, K., Valenzuela, R., Wang, C., Rester, L., Beaulieu, A., 2024. South America is becoming warmer, drier, and more flammable. Commun. Earth Environ. 5, 501.
Field, R.D., 2020. Evaluation of global fire weather database reanalysis and short-term forecast products. Nat. Hazards Earth Syst. Sci. 20 (4), 1123–1147.
Galizia, L.F., Curt, T., Barbero, R., Rodrigues, M., 2022. Understanding fire regimes in Europe. Int. J. Wildland Fire 31, 56–66.
Gallo, C., Eden, J.M., Dieppois, B., Drobyshev, I., Fulé, P.Z., San-Miguel-Ayanz, J., Blackett, M., 2023. Evaluation of CMIP6 model performances in simulating fire weather spatiotemporal variability on global and regional scales. Geosci. Model Dev. 16, 3103–3122. https://doi.org/10.5194/gmd-16-3103-2023.
Giorgetta, M.A., Jungclaus, J., Reick, C.H., Legutke, S., Bader, J., Böttinger, M., Brovkin, V., Crueger, T., Esch, M., Fieg, K., Glushak, K., Gayler, V., Haak, H., Hollweg, H.-D., Ilyina, T., Kinne, S., Kornblueh, L., Matei, D., Mauritsen, T., Mikolajewicz, U., Mueller, W., Notz, D., Pithan, F., Raddatz, T., Rast, S., Redler, R., Roeckner, E., Schmidt, H., Schnur, R., Segschneider, J., Six, K.D., Stockhause, M., Timmreck, C., Wegner, Widmann, H., Wieners, K.-H., Claussen, M., Marotzke, J., Stevens, B., 2013. Climate and carbon cycle changes from 1850 to 2100 in MPI-ESM simulations for the coupled model intercomparison project phase 5. J. Adv. Model. Earth Syst. 5, 572–597. https://doi.org/10.1002/jame.20038.
Goss, M., Swain, D.L., Abatzoglou, J.T., Kolden, C.A., Williams, A.P., Diffenbaugh, N.S., 2020. Climate change is increasing the likelihood of extreme autumn wildfire conditions across California. Environ. Res. Lett. 15, 9. https://doi.org/10.1088/1748-9326/ab83a7.
Hetzer, J., Forrest, M., Ribalaygua, J., Prado-López, C., Hickler, T., 2024. The fire weather in Europe: Large-scale trends towards higher danger. Environ. Res. Lett. 19, 084017.
Hirsch, R.M., Slack, J.R., 1984. A nonparametric trend test for seasonal data with serial dependence. Water Resour. Res. 20 (6), 727–732.
Horing, J., Shivaram, R., Azevedo, I.M.L., 2025. Perceptions of wildfire risk and adaptation behaviour in California. Environ. Res. Clim. 4, 015010. https://doi.org/10.1088/2752-5295/ada8ca.
Jain, P., Tye, M.R., Paimazumder, D., Flannigan, M., 2020. Downscaling fire weather extremes from historical and projected climate models. Clim. Change 163, 189–216. https://doi.org/10.1007/s10584-020-02865-5.
Jain, P., Castellanos-Acuna, D., Coogan, S.C.P., Abatzoglou, J.T., Flannigan, M., 2022. Observed increases in extreme fire weather driven by atmospheric humidity and temperature. Nat. Clim. Change 12, 63–70. https://doi.org/10.1038/s41558-021-01224-1.
Kumar, A., Kumar, S., Rautela, K.S., Shekhar, S., Ray, T., Thangavel, M., 2023a. Assessing seasonal variation and trends in rainfall patterns of Madhya Pradesh. Central India, J. Water Clim. Change 14 (10), 3692–3712.
Kumar, A., Kumar, S., Rautela, K.S., Kumari, A., Shekhar, S., Thangavel, M., 2023b. Exploring temperature dynamics in Madhya Pradesh: A spatial-temporal analysis. Environ. Sci. Pollut. Res. 195, 1313. https://doi.org/10.1007/s10661-023-11884-5.
Kumar, A., Ray, T., Mohanasundari, T., 2024. Exploring climatic dynamics in Madhya Pradesh, India utilizing long-term gridded data (1951–2021): An integrated statistical and GIS modules. In: Yadav, A.K., Yadav, K., Singh, V.P. (Eds.), Integrated Management of Water Resources in India: A Computational Approach, vol. 129. Water Science and Technology Library, Springer, Cham, pp. 2–21.
Kumar, A., Thangavel, M., 2025. Unravelling the dynamics of rainfall patterns in Bihar, India: A comprehensive spatiotemporal analysis. Environ. Sci. Pollut. Res. 32, 8564–8584.
Leonardos, L., Gnilke, A., Sanders, T.G.M., Shatto, C., Stadelmann, C., Beierkuhnlein, C., Jentsch, A., 2024. Synthesis and perspectives on disturbance interactions, and forest fire risk and fire severity in Central Europe. Fire 7 (12), 470. https://doi.org/10.3390/fire7120470.
McBride, L.A., Hope, A.P., Canty, T.P., Bennett, B.F., Tribett, W.R., Salawitch, R.J., 2021. Comparison of CMIP6 historical climate simulations and future projected warming to an empirical model of global climate. Earth Syst. Dyn. 12, 545–579. https://doi.org/10.5194/esd-12-545-2021.
Miller, J., Böhnisch, A., Ludwig, R., Brunner, M.I., 2024. Climate change impacts on regional fire weather in heterogeneous landscapes of central Europe. Nat. Hazards Earth Syst. Sci. 24, 411–428. https://doi.org/10.5194/nhess-24-411-2024.
Mosha, N.S., Semgomba, D.S., Ntigwaza, C.Y., Masunga, D.J., 2025. Physical origins of spatial pattern of summer extreme high temperature days over northern Africa. J. Geosci. Environ. Protect. 13, 32–50.
Pinto, M.M., DaCamara, C.C., Hurduc, A., Trigo, R.M., Trigo, I.F., 2020. Enhancing the fire weather index with atmospheric instability information. Environ. Res. Lett. 15, 0940b7.
Richardson, D., Ribeiro, A.F.S., Batibeniz, F., Quilcaille, Y., Taschetto, A.S., Pitman, A.J., Zscheischler, J., 2025. Increasing fire weather season overlap between North America and Australia challenges firefighting cooperation. Earth's Future 13, e2024EF005030.
Rovithakis, A., Grillakis, M.G., Seiradakis, K.D., 2022. Future climate change impact on wildfire danger over the Mediterranean: The case of Greece. Environ. Res. Lett. 17, 045022. https://doi.org/10.1088/1748-9326/ac5f94.
Senande-Rivera, M., Insua-Costa, D., Miguez-Macho, G., 2025. Climate change aggravated wildfire behaviour in the Iberian Peninsula in recent years. Npj Clim. Atmos. Sci. 8, 19. https://doi.org/10.1038/s41612-025-00906-3.
Tomašević, I.Č., Cheung, K.K.W., Vučetić, V., Fox-Hughes, P., 2022. Comparison of wildfire meteorology and vlimate at the Adriatic coast and southeast Australia. Atmosphere. 13 (5), 755. https://doi.org/10.3390/atmos13050755.
Varela, V., Vlachogiannis, D., Sfetsos, A., Karozis, S., Politi, N., Giroud, F., 2019. Projection of forest fire danger due to climate change in the french Mediterranean region. Sustainability 11 (16), 4284. https://doi.org/10.3390/su11164284.
Voldoire, A., Sanchez-Gomez, E., Salas y Mélia, D., Decharme, B., Cassou, C., Sénési, S., Valcke, S., Beau, I., Alias, A., Chevallier, M., Déqué, M., Deshayes, J., Douville, H., Fernandez, E., Madec, G., Maisonnave, E., Moine, M.-P., Planton, S., Saint-Martin, D., Szopa, S., Tyteca, S., Alkama, R., Belamari, S., Braun, A., Coquart, L., Chauvin, F., 2013. The CNRM-CM5.1 global climate model: description and basic evaluation. Clim. Dyn. 40, 2091–2121. https://doi.org/10.1007/s00382-011-1259-y.
Zaidi, A., 2023. Predicting wildfires in Algerian forests using machine learning models. Heliyon 9 (7), e18064. https://doi.org/10.1016/j.heliyon.2023.e18064.